Available online at www.sciencedirect.com
ScienceDirect
Physica A 385 (2007) 558–572
PHYSICA A
www.elsevier.com/locate/physa

Thermodynamic variables of microquasars inferred from tachyonic spectral maps

Roman Tomaschitz*

Department of Physics, Hiroshima University, 1-3-1 Kagami-yama, Higashi-Hiroshima 739-8526, Japan

Received 28 September 2006; received in revised form 4 June 2007
Available online 13 June 2007

Abstract

Tachyonic spectral densities of ultra-relativistic electron populations are fitted to the γ-ray spectra of two microquasars, LS 5039 and LSI $+61°303$. The superluminal spectral maps are obtained from BATSE, COMPTEL, EGRET, HESS, and MAGIC data sets. The spectral averaging is done with exponentially cut power-law densities. Estimates of the electron distributions generating the tachyon flux are obtained from the spectral fits, such as power-law indices, electron temperature and source counts. The internal energy and heat capacities of the source populations are calculated. An extensive entropy functional is defined for Boltzmann power-law densities and its stability is checked. The high-temperature limit of the thermodynamic variables is determined by the power-law index of the electron plasma, which enters in the scaling exponents as well as the amplitudes.

PACS: 05.70.Ce; 05.20.Gg; 52.25.Kn; 95.30.Tg

Keywords: Superluminal radiation; Tachyonic γ-rays; Boltzmann power-law ensembles; Spectral averaging; γ-Ray binaries

1. Introduction

We study the tachyonic spectral maps of two microquasars, LS 5039, cf. Refs. [1,2], and LSI $+61°303$, cf. Refs. [3,4], and reconstruct the electron distributions emitting the superluminal radiation. The spectral maps of these γ-ray binaries suggest cascade spectra which are generated by electronic power-law densities exponentially cut with the Boltzmann factor. Classical statistics applies, as the high-temperature regime is invoked at γ-ray energies. We average the tachyonic spectral densities with electronic power-law distributions, and infer the power-law index, the electron count, and the temperature from the spectral fits. Based on these parameters, we calculate the internal energy and the specific heat of the ultra-relativistic electron plasma of the microquasars. To this end, we set up the thermodynamic formalism for Boltzmann power-law ensembles. Starting with the grand partition function, we find an entropy functional for exponentially cut power-law densities that is extensive and stable. We derive the Helmholtz and Gibbs free energies as well as the low- and

*Tel.: +81 824 247361; fax: +81 824 240717.
E-mail address: tom@geminga.org

0378-4371/$ - see front matter © 2007 Elsevier B.V. All rights reserved.
doi:10.1016/j.physa.2007.06.009

high-temperature expansions of the caloric equation of state and the heat capacities, in particular their high-temperature scaling depending on the electronic power-law index.

In Section 2, we briefly sketch the transversal and longitudinal tachyonic spectral densities and their averaging with Boltzmann power laws, which results in cascade spectra. We perform the spectral fits to the γ-ray wideband of the microquasars, and extract the parameters of the electronic source populations, such as power-law index, temperature and source number. In Section 3, we develop the thermodynamic formalism for exponentially cut power-law densities and derive the low- and high-temperature expansions of the thermodynamic variables, focusing on entropy, equations of state, and the specific heats. In Section 4, we investigate ultra-relativistic Boltzmann ensembles, power-law densities with Lorentz factors exceeding a high-energy threshold, and we calculate the internal energy and heat capacities of the electron gas in the two microquasars. In Section 5, we present our conclusions. In Appendix A, we list the asymptotic expansions of the partition function, entropy, and the free energies at integer electronic spectral index, which requires special treatment due to logarithmic temperature dependence in the high-temperature regime.

2. Tachyonic γ-ray spectra of microquasars

The tachyonic radiation densities of uniformly moving electrons were derived in Ref. [5],

$$p^{\mathrm{T,L}}(\omega,\gamma)=\frac{\alpha_q m_{\mathrm{t}}^2\omega}{\omega^2+m_{\mathrm{t}}^2}\left[\gamma^2-\left(1+\frac{\omega^2}{m_{\mathrm{t}}^2}\right)\Delta^{\mathrm{T,L}}\right]\frac{1}{\gamma\sqrt{\gamma^2-1}}, \tag{2.1}$$

where $\Delta^{\mathrm{T}}=1$ refers to the transversal superluminal radiation, and $\Delta^{\mathrm{L}}=0$ holds for the longitudinal component. We use the classical limit of the radiation densities, neglecting terms depending on the electron–tachyon mass ratio, as the spectral fits are done in the ultra-relativistic high-temperature regime [6]; γ denotes the electronic Lorentz factor, α_q the tachyonic fine structure constant, and m_{t} the tachyon mass. The spectral cutoff occurs at $\omega_{\max}(\gamma):=m_{\mathrm{t}}\sqrt{\gamma^2-1}$. Only frequencies in the range $0<\omega<\omega_{\max}(\gamma)$ can be radiated by a uniformly moving charge; the tachyonic spectral densities $p^{\mathrm{T,L}}(\omega)$ are cut off at the break frequency $\omega_{\max}$. We use the Heaviside–Lorentz system, so that $\alpha_q=q^2/(4\pi\hbar c)\approx 1.0\times 10^{-13}$. The tachyon mass is $m_{\mathrm{t}}\approx 2.15\,\mathrm{keV}/c^2$, and the tachyon–electron mass ratio $m_{\mathrm{t}}/m\approx 1/238$. These estimates are obtained from hydrogenic Lamb shifts [7].

The radiation densities (2.1) refer to a single charge with Lorentz factor γ. We average them with ultra-relativistic electron distributions, power-law densities exponentially cut with the Boltzmann factor:

$$\mathrm{d}\rho_{\alpha,\beta}(\gamma)=A_{\alpha,\beta}\gamma^{-\alpha-1}\mathrm{e}^{-\beta\gamma}\sqrt{\gamma^2-1}\,\mathrm{d}\gamma. \tag{2.2}$$

The electronic Lorentz factors range in an interval $\gamma_1\leqslant\gamma<\infty$. The normalization $A_{\alpha,\beta}$ is determined by $n_1=\int_{\gamma_1}^{\infty}\mathrm{d}\rho_{\alpha,\beta}(\gamma)$, where n_1 is the electron count and $\gamma_1\gg 1$ the lower edge of Lorentz factors in the source population. The exponential cutoff is related to the electron temperature by $\beta=mc^2/(kT)$, and α is the electronic power-law index. When discussing the thermodynamics of Boltzmann power-law ensembles, we will redefine the power-law index as $\delta=\alpha+2$, so that a thermal Maxwell–Boltzmann distribution corresponds to $\delta=0$ and $\gamma_1=1$. In spectral averages it is customary to define the electron index by α as done in Eq. (2.2). The average is carried out as [6]

$$\langle p^{\mathrm{T,L}}(\omega)\rangle_{\alpha,\beta}:=\int_{\gamma_1}^{\infty}p^{\mathrm{T,L}}(\omega,\gamma)\theta(\omega_{\max}(\gamma)-\omega)\,\mathrm{d}\rho_{\alpha,\beta}(\gamma), \tag{2.3}$$

and the spectral fit is based on the E^2-rescaled flux densities:

$$E^2\frac{\mathrm{d}N^{\mathrm{T,L}}}{\mathrm{d}E}=\frac{\omega}{4\pi d^2}\langle p^{\mathrm{T,L}}(\omega)\rangle_{\alpha,\beta}, \tag{2.4}$$

where d is the distance to the source. The spectral maps of the microquasars in Figs. 1–3 are fitted with the unpolarized flux density $\mathrm{d}N^{\mathrm{T+L}}=\mathrm{d}N^{\mathrm{T}}+\mathrm{d}N^{\mathrm{L}}$ of electron populations $\rho_{i=1,2}$ specified in Table 1. Each electron density generates a cascade ρ_i, and the wideband fit is obtained by adding two cascade spectra, labeled ρ_1 and ρ_2 in the figures.

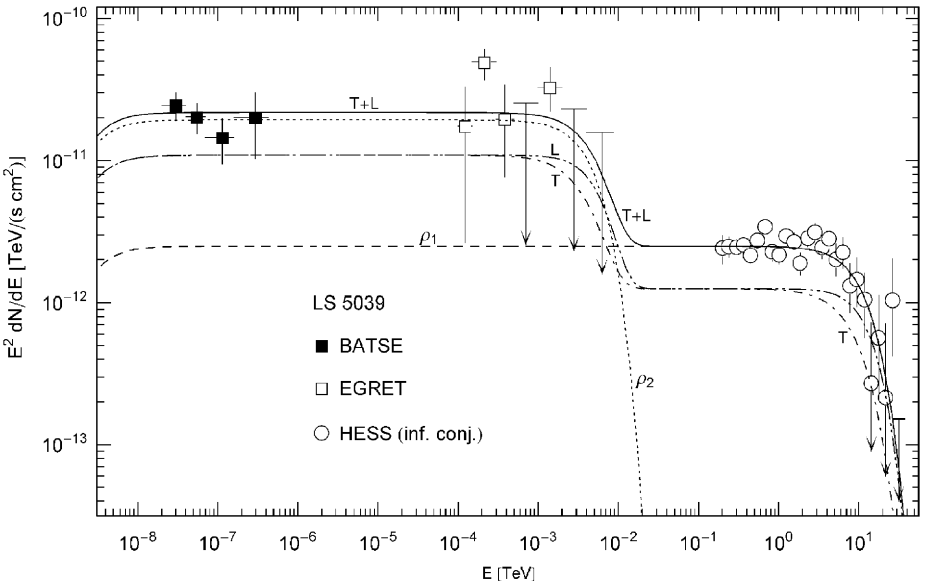

Fig. 1. γ-Ray wideband of the microquasar LS 5039. BATSE data points from Ref. [8], EGRET points from Refs. [9,10], and HESS points from Ref. [11]. BATSE and EGRET data refer to the associated EGRET source 3EG J1824 − 1514, HESS points to HESS J1826 − 148 at the inferior conjunction as defined in Ref. [11]. The solid line T + L depicts the unpolarized differential tachyon flux dN^{T+L}/dE, obtained by adding the flux densities $\rho_{1,2}$ of two electron populations and rescaled with E^2 for better visibility of the spectral curvature, cf. (2.4). The transversal (T, dot-dashed) and longitudinal (L, double-dot-dashed) flux densities $dN^{T,L}/dE$ add up to the total flux T + L. The exponential decay of the cascades $\rho_{1,2}$ sets in at about $E_{cut} \approx (m_t/m)kT$, implying cutoffs at 5 TeV for the ρ_1 cascade and at 2 GeV for ρ_2, which terminate the spectral plateaus. The unpolarized flux T + L is the actual spectral fit, the parameters of the electron densities are recorded in Table 1.

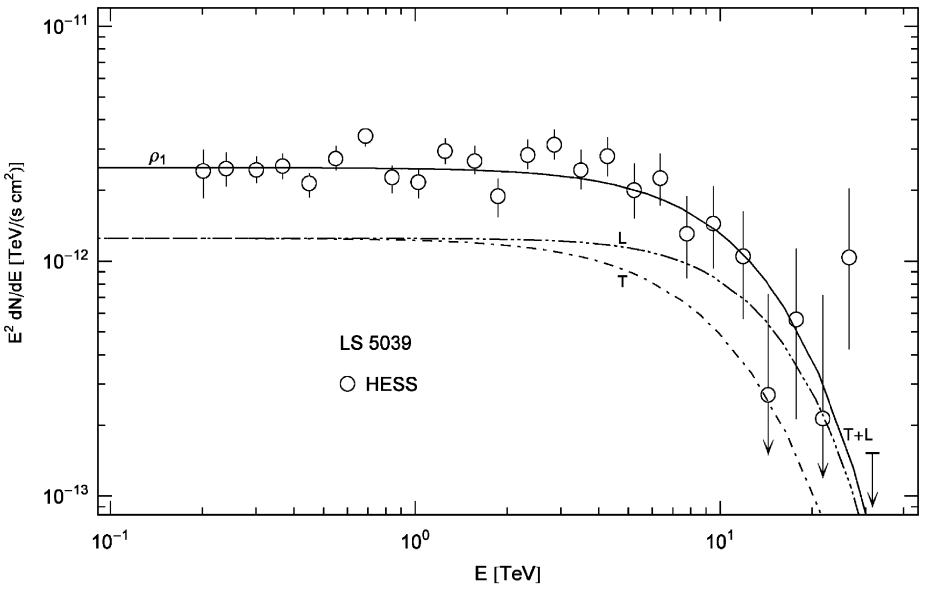

Fig. 2. Close-up of the HESS spectrum of LS 5039 in Fig. 1. The TeV spectral map coincides with the ρ_1 cascade, since the ρ_2 flux is exponentially cut at 2 GeV. T and L stand for the transversal and longitudinal flux components, and T + L labels the unpolarized flux. The HESS points define a spectral plateau in the high GeV range typical for cascade spectra, followed by exponential decay. The spectral curvature is generated by the Boltzmann factor in the electron densities. If rescaled, this spectral map is quite similar to the cascade spectra of the Markarian galaxies Mkn 501 and Mkn 421 in Figs. 5 and 6 of Ref. [6].

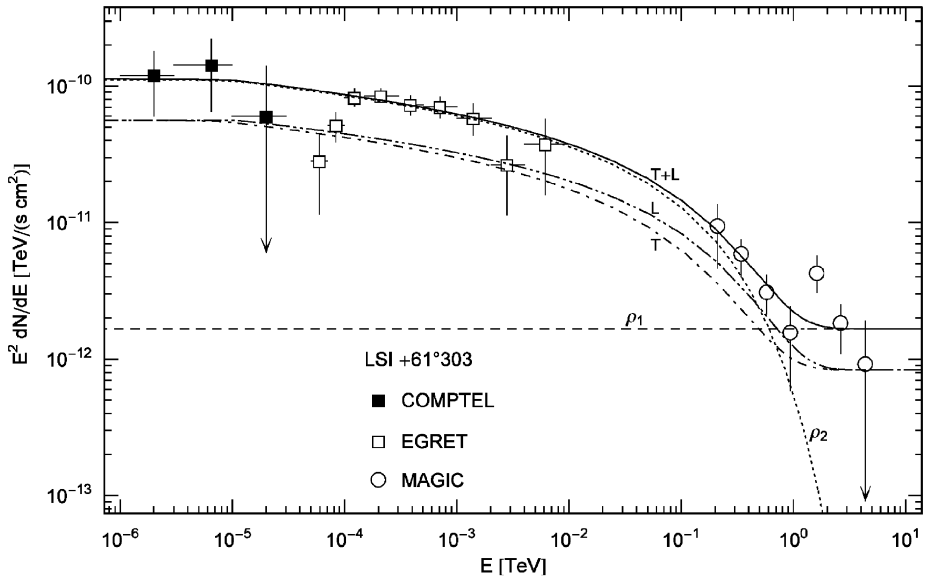

Fig. 3. Spectral map of the microquasar LSI +61°303, associated with the EGRET source 3EG J0241+6103. COMPTEL points from Ref. [12], EGRET data from Refs. [13,14], and MAGIC points from Ref. [15]. The plots are labeled as in Fig. 1. The χ^2-fit is done with the total unpolarized tachyon flux T+L and subsequently split into transversal (dot-dashed) and longitudinal (double-dot-dashed) components. A spectral break at $m_t\gamma_1 \approx 11\,\mathrm{MeV}$ is visible as edge in the spectral map; exponential decay sets in at the cutoff frequency $E_{\mathrm{cut}} \approx 0.6\,\mathrm{TeV}$. In the extended crossover regime between the spectral break and the spectral cutoff, the decay is gradual but not power law, with electron index $\alpha = 1$. (A power-law crossover, $E^2\,\mathrm{d}N^{\mathrm{T+L}}/\mathrm{d}E \propto E^{1-\alpha}$, occurs for electron indices $\alpha > 1$, cf. Ref. [6]).

Table 1
Electronic source densities $\rho_{1,2}$ generating the γ-ray broadband of the microquasars LS 5039 and LSI +61°303

	α	β	γ_1	$\hat{n}$	n^{e}	kT (TeV)
LS 5039					@2.5 kpc	
ρ_1	−2	4.39×10^{-10}	1	2.7×10^{-4}	9.7×10^{46}	1160
ρ_2	−2	1.075×10^{-6}	1	2.1×10^{-3}	7.6×10^{47}	0.475
LSI +61°303					@2 kpc	
ρ_1	−2	—	1	1.8×10^{-4}	4.1×10^{46}	—
ρ_2	1	3.77×10^{-9}	5.0×10^{3}	1.2×10^{-2}	2.8×10^{48}	136

Each ρ_i stands for a Boltzmann power-law density $\mathrm{d}\rho_{\alpha,\beta}(\gamma)$ defined by parameters $(\alpha,\beta,\gamma_1,\hat{n})$, cf. (2.2). α is the electronic power-law index, $\beta = mc^2/(kT)$ the cutoff parameter in the Boltzmann factor, and γ_1 the lower edge of Lorentz factors in the electronic source population ρ_i. The amplitude of the tachyon flux generated by ρ_i is determined by $\hat{n}$, from which the electron count n^{e} is inferred at the indicated distance, cf. (2.5). (The subscript 1 in $\hat{n}$ and n^{e} has been dropped). kT is the electron temperature. In the thermodynamic variables, we identify $\delta = \alpha + 2$ and put $N = n^{\mathrm{e}}$, cf. Sections 3 and 4. The cascades labeled ρ_i in Figs. 1–3 are obtained by averaging the tachyonic radiation densities (2.1) with the electron distributions ρ_i, cf. (2.3) and (2.4). The parameters α, β, γ_1, and $\hat{n}$ are extracted from the least-squares fit T+L in the figures. As for the thermal high-energy population ρ_1 of LSI +61°303, it is not yet possible to determine the spectral cutoff and the electron temperature from the presently available TeV data.

As for the electron count n_1, we use a rescaled parameter $\hat{n}_1$ for the fit:

$$\hat{n}_1 := \frac{\alpha_q n_1}{\hbar[\mathrm{keV\,s}]4\pi d^2[\mathrm{cm}]} \approx 1.27\times10^{-39}\frac{n_1}{d^2[\mathrm{kpc}]}, \tag{2.5}$$

which is independent of the distance estimate. Here, $\hbar$[keV s] implies the tachyon mass in keV units, that is, we put $m_t \approx 2.15$ in the spectral density (2.1). At γ-ray energies, only a tiny α_q/α_e-fraction (the ratio of tachyonic and electric fine structure constants) of the tachyon flux is absorbed by the detector, which requires a rescaling of the electron count n_1, so that the actual number of radiating electrons is $n_1^{\mathrm{e}} := n_1\alpha_e/\alpha_q \approx 7.3\times10^{10}n_1$.

We thus find the electron count as $n_1^e \approx 5.75\times 10^{49}\hat{n}_1 d^2$[kpc], where $\hat{n}_1$ defines the tachyonic flux amplitude extracted from the spectral fit [6,7]. As for electron temperature and cutoff parameter in the Boltzmann factor, we note kT[TeV] $\approx 5.11\times 10^{-7}/\beta$. The electronic source count for the Crab pulsar at $d\approx 2$ kpc is 2.6×10^{49}, cf. Ref. [16], as compared to 8.6×10^{47} for LS 5039 and 2.8×10^{48} for LSI $+61^\circ 303$; these estimates are obtained by adding the source counts of the high- and low-energy populations $\rho_{1,2}$ in Table 1. A similar source number of 3.2×10^{47} was derived in Ref. [17] for the binary pulsar PSR B1259 − 63 at 1.5 kpc, which suggests a neutron star as compact companion in both microquasars.

In Figs. 1 and 2, we depict the spectral map of the microquasar LS 5039, located at a distance of 2.5 kpc, a compact object orbiting a massive O-star [8–11]. Mass estimates and orbital parameters are given in Refs. [1,2]; we do not list them here, as they are not required to infer the thermodynamic parameters of the electron plasma. LS 5039 is associated with the unidentified EGRET source 3EG J1824 − 1514 and the TeV source HESS J1826 − 148, cf. Refs. [11,18]. The tachyonic spectral maps are further explained in the figure captions. The GeV spectrum in Fig. 1 can be compared to the spectral map in Fig. 2 of Ref. [10], based on inverse Compton scattering.

Fig. 3 shows the tachyonic spectral map of the microquasar LSI $+61^\circ 303$, at $d\approx 2$ kpc, associated with the unidentified EGRET source 3EG J0241 + 6103, cf. Refs. [12–15,19,20]. Estimates of the orbital parameters of this binary system, a massive Be star with a compact companion, are given in Refs. [3,4]. Inverse-Compton fits of the EGRET spectrum can be found in Figs. 2–4 of Ref. [14]. The thermodynamic variables of the electron populations are discussed in Section 3, and estimates of the internal energy and the specific heats are derived in Section 4. The spectral fits in Figs. 1–3 are performed with the unpolarized tachyon flux. At γ-ray energies, the speed of tachyons is close to the speed of light, the basic difference to electromagnetic radiation being the longitudinal flux component. The polarization of tachyons can be determined from transversal and longitudinal ionization cross-sections [21,22].

3. Caloric equation of state and heat capacities of electronic power-law distributions

The exponentially cut power-law distribution (2.2) is obtained from the momentum-space density $\mathrm{d}\rho \propto H^{-\delta}\mathrm{e}^{-H/(kT)}\mathrm{d}^3p$, where $H = m\gamma$ is the free Hamiltonian, and the electronic Lorentz factors range in the interval $\gamma_1 \leqslant \gamma < \infty$. The power-law exponent δ is related to the electron index in Eq. (2.2) by $\delta = \alpha + 2$. The thermodynamic formalism employed is standard, and no derivations are given, although we will consider stability conditions such as the positivity of the specific heat and compressibility. We will discuss the low- and high-temperature expansions of the caloric equation of state and the isochoric heat capacity, in particular their qualitative dependence on the power-law index δ. The typical range of δ in spectral averages is narrow, very rarely outside the interval $0\leqslant\delta\leqslant 4$, cf. Refs. [23–31]. The relativistic thermal Maxwell–Boltzmann distribution in 3D is recovered with $\delta = 0$ and $\gamma_1 = 1$, cf. Ref. [32]. Here, we will study power-law ensembles with arbitrary real index δ.

We start with the classical grand partition function

$$Z = \sum_{n=0}^{\infty}\frac{1}{n!}\left(\int_V\int_{R^3}\rho\,\frac{\mathrm{d}^3p\,\mathrm{d}^3q}{(2\pi)^3}\right)^n, \tag{3.1}$$

with density

$$\rho = (H/m)^{-\delta}\,\exp(-\beta H/m - \alpha), \tag{3.2}$$

where $H/m = \gamma$ and $\beta = m/(kT)$. The thermal wavelength reads $\lambda_T = \sqrt{2\pi\beta}/m$, and $\lambda_T^3 N/V \ll 1$ is required for classical statistics to apply. We parametrize the momentum integration in Eq. (3.1) with the Lorentz factor, $p = m\sqrt{\gamma^2-1}$, and perform the angular integration, so that $\mathrm{d}^3p = 4\pi m^3\sqrt{\gamma^2-1}\gamma\,\mathrm{d}\gamma$. In the ultra-relativistic limit, $p\sim m\gamma$, the factor $\gamma^{-\delta}$ in density (3.2) can be generated by analytic continuation in the space dimension. The fact that the exponent δ varies only in a narrow range also suggests treating it like a dimension rather than an intensive variable when setting up the thermodynamic formalism for power-law ensembles. We find

$$\int_{R^3}\rho\,\mathrm{d}^3p = 4\pi m^3\mathrm{e}^{-\alpha}K(\delta,\beta), \tag{3.3}$$

where

$$K(\delta,\beta) := \int_1^\infty \sqrt{\gamma^2-1}\gamma^{1-\delta}\mathrm{e}^{-\beta\gamma}\,\mathrm{d}\gamma. \tag{3.4}$$

The momentum integration (3.3) is over R^3, as we at first consider the full range of Lorentz factors, $1\leqslant\gamma<\infty$. In Section 4, we will discuss a truncated electron density, restricting the integration range in Eq. (3.3) to $H\geqslant H_1=m\gamma_1$, $\gamma_1>1$, which amounts to replacing the lower integration boundary in Eq. (3.4) by γ_1; in particular, we will study ultra-relativistic ensembles with high-energy threshold $\gamma_1\gg 1$. In this section, we assume $\gamma_1=1$.

The summation in Eq. (3.1) gives

$$\log Z = \frac{m^3V}{2\pi^2}\mathrm{e}^{-\alpha}K(\delta,\beta), \tag{3.5}$$

and we find the internal energy and the particle number as

$$U = -m\frac{\partial}{\partial\beta}\log Z = -\frac{m^4V}{2\pi^2}\mathrm{e}^{-\alpha}\frac{\partial K(\delta,\beta)}{\partial\beta}, \tag{3.6}$$

$$N = -\frac{\partial}{\partial\alpha}\log Z = \frac{m^3V}{2\pi^2}\mathrm{e}^{-\alpha}K(\delta,\beta). \tag{3.7}$$

Here, m^3V is dimensionless, so that $m\to mc/\hbar$ when restoring units, and $\beta=mc^2/(kT)$. On eliminating the fugacity $\mathrm{e}^{-\alpha}$, we obtain the caloric equation of state:

$$U(\delta,\beta,N) = -mN\frac{\partial}{\partial\beta}\log K(\delta,\beta). \tag{3.8}$$

The chemical potential reads

$$\mu(\delta,\beta,V,N) = -m\frac{\alpha}{\beta},\quad \alpha=\log\left(\frac{m^3V}{2\pi^2N}K(\delta,\beta)\right), \tag{3.9}$$

and the entropy is defined as

$$S = k\left(\log Z+\beta\frac{U}{m}+\alpha N\right). \tag{3.10}$$

By making use of $N=\log Z$, we find

$$S(\delta,\beta,V,N) = kN\left[1+\log\left(\frac{m^3V}{2\pi^2N}K(\delta,\beta)\right)-\beta\frac{\partial}{\partial\beta}\log K(\delta,\beta)\right]. \tag{3.11}$$

The homogeneity relation, $S/N=S(\delta,\beta,V/N,1)$, is satisfied, and we may substitute $\beta(U/N)$ by solving (3.8).

We note the Helmholtz free energy $U-TS$,

$$F(\delta,\beta,V,N) = -\frac{mN}{\beta}\left[1+\log\left(\frac{m^3V}{2\pi^2N}K(\delta,\beta)\right)\right], \tag{3.12}$$

and the thermal equation of state, $P=-\partial F/\partial V$ or $PV=mN/\beta$. The isochoric specific heat reads

$$C_V = -\beta\frac{\partial}{\partial\beta}S(\delta,\beta,V,N) = kN\beta^2\frac{\partial^2}{\partial\beta^2}\log K(\delta,\beta). \tag{3.13}$$

This is the energy required to shift the exponential cutoff of the power-law slope, that is, to vary the electron temperature without changing volume and power-law index. The isothermal compressibility is

$$\kappa_T = -\frac{1}{V}\frac{\partial}{\partial P}V(\delta,\beta,P,N) = \frac{1}{P}. \tag{3.14}$$

Thermodynamic stability, $\mathrm{d}^2S\leqslant 0$ at $\mathrm{d}S=0$ (with δ kept fixed) requires $C_V\geqslant 0$ and $\kappa_T\geqslant 0$, the latter is obviously satisfied. As for the first, we note $\partial K(\delta,\beta)/\partial\beta=-K(\delta-1,\beta)$ and the Schwarz inequality

$K^2(\delta-1,\beta)<K(\delta,\beta)K(\delta-2,\beta)$, which implies $C_V>0$. As for energy and number fluctuations, we note the variances

$$(\Delta U)^2=\frac{m^2}{k\beta^2}C_V,\quad (\Delta N)^2=\frac{mN^2}{\beta V}\kappa_T=N, \tag{3.15}$$

which result in $1/\sqrt{N}$ decay of the fluctuations $\Delta U/U$ and $\Delta N/N$. The isobaric expansivity is

$$\alpha_P=-\frac{k\beta^2}{mV}\frac{\partial}{\partial\beta}V(\delta,\beta,P,N)=\frac{k}{m}\beta, \tag{3.16}$$

where $mc^2/k\approx 5.930\times 10^9\,\mathrm{K}$, and the isobaric heat capacity C_P is calculated by means of the identity

$$C_P-C_V=\frac{mV}{k\beta}\frac{\alpha_P^2}{\kappa_T}=kN. \tag{3.17}$$

The adiabatic compressibility and the adiabatic expansion coefficient read

$$\kappa_S=-\frac{1}{V}\frac{\partial}{\partial P}V(\delta,S,P,N),\quad \alpha_S=-\frac{k\beta^2}{mV}\frac{\partial}{\partial\beta}V(\delta,\beta,S,N), \tag{3.18}$$

and are calculated via the identities [33]

$$\frac{\kappa_S}{\kappa_T}=\frac{1}{\gamma_C},\quad \frac{\alpha_S}{\alpha_P}=\frac{1}{1-\gamma_C}, \tag{3.19}$$

where γ_C denotes the heat capacity ratio C_P/C_V. The positivity conditions $C_V>0$ and $\kappa_T>0$ thus imply $C_P>C_V$, $\gamma_C>1$, and $\kappa_T>\kappa_S>0$; the adiabatic expansivity α_S is negative.

The low-temperature expansion of the equation of state (3.8) reads

$$\frac{U-mN}{mN}=\frac{3}{2}\frac{1}{\beta}-\frac{1}{\beta^2}\frac{3}{2}\left(\delta-\frac{5}{4}\right)+\frac{1}{\beta^3}\frac{3}{2}\left(\delta^2-\frac{5}{4}\right)+\ldots \tag{3.20}$$

As for the heat capacities at constant volume/pressure, we use (3.13) to find

$$\frac{C_V}{kN}=\frac{3}{2}-\frac{3}{\beta}\left(\delta-\frac{5}{4}\right)+\frac{1}{\beta^2}\frac{9}{2}\left(\delta^2-\frac{5}{4}\right)+\ldots,\quad \frac{C_P}{kN}=1+\frac{C_V}{kN}. \tag{3.21}$$

The leading order is just the non-relativistic result; at low temperature, the power-law index enters only into the relativistic corrections. Here and in the following, the asymptotic expansions are obtained by term-by-term differentiation of the $\log K$ series in Appendix A.

The high-temperature expansions of the internal energy and the isochoric specific heat differ qualitatively in different δ ranges. We define the coefficients

$$c_k(\delta):=\frac{\sqrt{\pi}}{4}\frac{\Gamma\big((\delta-3-k)/2\big)}{\Gamma\big((\delta-k)/2\big)}, \tag{3.22}$$

and find, for $\delta<1$,

$$\frac{U}{mN}=\frac{3-\delta}{\beta}+\frac{\beta}{(2-\delta)(1-\delta)}+\mathrm{O}(\beta^3,\beta^{2-\delta}),\quad \frac{C_V}{kN}=3-\delta-\frac{\beta^2}{(2-\delta)(1-\delta)}+\mathrm{O}(\beta^4,\beta^{3-\delta}). \tag{3.23}$$

In the range $1<\delta<3$, the next-to-leading order is modified as

$$\frac{U}{mN}=\frac{3-\delta}{\beta}-\frac{(3-\delta)c_0(\delta)}{\Gamma(3-\delta)}\beta^{2-\delta}+\mathrm{O}(\beta,\beta^{5-2\delta}),\quad \frac{C_V}{kN}=3-\delta+\frac{(3-\delta)c_0(\delta)}{\Gamma(2-\delta)}\beta^{3-\delta}+\mathrm{O}(\beta^2,\beta^{2(3-\delta)}). \tag{3.24}$$

In the interval $3<\delta<4$, we obtain

$$\frac{U}{mN}=\frac{\Gamma(4-\delta)}{c_0(\delta)}\beta^{\delta-4}+\frac{c_1(\delta)}{c_0(\delta)}-\frac{\Gamma(3-\delta)\Gamma(4-\delta)}{c_0^2(\delta)}\beta^{2\delta-7}+\mathrm{O}(\beta^{\delta-3}),$$
$$\frac{C_V}{kN}=\frac{\Gamma(5-\delta)}{c_0(\delta)}\beta^{\delta-3}+\frac{\Gamma(3-\delta)\Gamma(4-\delta)}{c_0^2(\delta)}(2\delta-7)\beta^{2(\delta-3)}+\mathrm{O}(\beta^{\delta-2}), \tag{3.25}$$

and for $4<\delta<5$

$$\frac{U}{mN}=\frac{c_1(\delta)}{c_0(\delta)}+\frac{\Gamma(4-\delta)}{c_0(\delta)}\beta^{\delta-4}+\mathrm{O}(\beta),\quad \frac{C_V}{kN}=\frac{\Gamma(5-\delta)}{c_0(\delta)}\beta^{\delta-3}+\mathrm{O}(\beta^2). \tag{3.26}$$

Finally, for $\delta>5$

$$\frac{U}{mN}=\frac{c_1(\delta)}{c_0(\delta)}-\beta\left(\frac{c_2(\delta)}{c_0(\delta)}-\frac{c_1^2(\delta)}{c_0^2(\delta)}\right)+\mathrm{O}(\beta^2,\beta^{\delta-4}),\quad \frac{C_V}{kN}=\left(\frac{c_2(\delta)}{c_0(\delta)}-\frac{c_1^2(\delta)}{c_0^2(\delta)}\right)\beta^2+\mathrm{O}(\beta^3,\beta^{\delta-3}). \tag{3.27}$$

The leading-order coefficients are all positive, which is easy to see except for C_V in Eq. (3.27), where positivity follows from the Schwarz inequality, cf. after (3.14). Regarding units, we note $k\approx 8.617\times 10^{-17}\,\mathrm{TeV/K}$ and $1\,\mathrm{TeV}\approx 1.602\,\mathrm{erg}$.

In the case of integer δ, there appear singularities in the expansion coefficients, which cancel if ε expanded, cf. Appendix A and Ref. [7]. We list the equation of state and the specific heat for integer power-law index $0\leqslant\delta\leqslant 5$. Outside this range, the indicated orders of expansions (3.23) and (3.27) are singularity free and can be used even at integer δ. As for the caloric equation, we find

$$\frac{U(\delta=0)}{mN}=\frac{3}{\beta}+\frac{\beta}{2}+\mathrm{O}(\beta^3\,\log\,\beta),\quad \frac{U(\delta=1)}{mN}=\frac{2}{\beta}-\beta\left(\log\frac{\beta}{2}+\gamma_{\mathrm{E}}\right)+\mathrm{O}(\beta^3\,\log\,\beta),$$
$$\frac{U(\delta=2)}{mN}=\frac{1}{\beta}+\frac{\pi}{2}+\beta\left(\log\frac{\beta}{2}+\gamma_{\mathrm{E}}-1+\frac{\pi^2}{4}\right)+\mathrm{O}(\beta^2\log\beta),$$
$$\frac{U(\delta=3)}{mN}=\frac{1}{\beta}\frac{1}{\log(2/\beta)-\gamma_{\mathrm{E}}-1}+\mathrm{O}\left(\frac{1}{\log\beta}\right),\quad \frac{U(\delta=4)}{mN}=\frac{4}{\pi}\left(\log\frac{2}{\beta}-\gamma_{\mathrm{E}}-1\right)+\mathrm{O}(\beta\log^2\beta),$$
$$\frac{U(\delta=5)}{mN}=\frac{3\pi}{4}+3\beta\left(\log\frac{\beta}{2}+\gamma_{\mathrm{E}}+\frac{3\pi^2}{16}\right)+\mathrm{O}(\beta^2\,\log\,\beta), \tag{3.28}$$

where $\gamma_{\mathrm{E}}\approx 0.5772$. The internal energy admits a finite high-temperature limit for power-law indices $\delta>4$. The enthalpy is $U+mN/\beta$. The high-temperature expansion of the corresponding isochoric heat capacity reads

$$\frac{C_V(\delta=0)}{kN}=3-\frac{1}{2}\beta^2+\mathrm{O}(\beta^4\,\log\,\beta),\quad \frac{C_V(\delta=1)}{kN}=2+\beta^2\left(\log\frac{\beta}{2}+\gamma_{\mathrm{E}}+1\right)+\mathrm{O}(\beta^4\,\log\,\beta),$$
$$\frac{C_V(\delta=2)}{kN}=1-\beta^2\left(\log\frac{\beta}{2}+\gamma_{\mathrm{E}}+\frac{\pi^2}{4}\right)+\mathrm{O}(\beta^3\,\log\,\beta),$$
$$\frac{C_V(\delta=3)}{kN}=\frac{\log(2/\beta)-\gamma_{\mathrm{E}}-2}{(\log(2/\beta)-\gamma_{\mathrm{E}}-1)^2}+\mathrm{O}\left(\frac{\beta}{\log^2\beta}\right),\quad \frac{C_V(\delta=4)}{kN}=\frac{4}{\pi}\beta+\mathrm{O}(\beta^2\log^2\beta),$$
$$\frac{C_V(\delta=5)}{kN}=3\beta^2\left(\log\frac{2}{\beta}-\gamma_{\mathrm{E}}-\frac{3\pi^2}{16}-1\right)+\mathrm{O}(\beta^3\,\log\,\beta). \tag{3.29}$$

The case $\delta=0$ is the high-temperature limit of a Maxwell–Boltzmann distribution [32]. The specific heat is safely positive, but approaches zero in the high-temperature limit for power-law indices $\delta\geqslant 3$.

4. Ultra-relativistic Boltzmann power laws

We proceed as in Section 3, but restrict the momentum integration in the partition function (3.1) to ultra-relativistic Lorentz factors, so that $p=m\sqrt{\gamma^2-1}$ with γ ranging above a high-energy edge $\gamma_1\gg 1$. In the

partition function (3.1), we substitute the truncated density

$$\rho_1 = \theta(H - H_1)(H/m)^{-\delta} \exp(-\beta H/m - \alpha), \tag{4.1}$$

where $H_1 = m\gamma_1$ is the threshold energy. The step function restricts the $\mathrm{d}^3p\mathrm{d}^3q$ integration in Eq. (3.1) to $H(p,q) \geqslant H_1$:

$$\int_{R^3} \rho_1 \,\mathrm{d}^3p = \int_{H\geqslant H_1} \rho \,\mathrm{d}^3p = 4\pi m^3 \mathrm{e}^{-\alpha} K(\delta,\beta,\gamma_1), \tag{4.2}$$

with density ρ in Eq. (3.2), so that

$$K(\delta,\beta,\gamma_1) := \int_{\gamma_1}^{\infty} \sqrt{\gamma^2-1}\,\gamma^{1-\delta}\mathrm{e}^{-\beta\gamma}\,\mathrm{d}\gamma. \tag{4.3}$$

Eqs. (3.5)–(3.19) remain valid with $K(\delta,\beta)$ replaced by $K(\delta,\beta,\gamma_1)$; internal energy and heat capacity read

$$\frac{U(\gamma_1)}{mN} = -\frac{\partial}{\partial\beta}\log K(\delta,\beta,\gamma_1), \tag{4.4}$$

$$\frac{C_V(\gamma_1)}{kN} = \beta^2\frac{\partial^2}{\partial\beta^2}\log K(\delta,\beta,\gamma_1). \tag{4.5}$$

Schwarz's inequality as stated after (3.14) also applies to $K(\delta,\beta,\gamma_1)$, so that the maximum condition $\mathrm{d}^2S \leqslant 0$ at fixed δ and γ_1 is met. The low-temperature expansion (3.20) of the internal energy is replaced by [7]

$$\frac{U(\gamma_1) - m\gamma_1 N}{mN} = \frac{1}{\beta}\left(1 + \frac{1-(\delta-1)\upsilon_1^2}{\beta\gamma_1\upsilon_1^2} + \mathrm{O}\left(\frac{1}{(\beta\gamma_1\upsilon_1^2)^2}\right)\right), \tag{4.6}$$

where $\upsilon_1^2 := 1 - 1/\gamma_1^2$. The asymptotic parameter is $\beta\gamma_1\upsilon_1^2 \gg 1$, so that this expansion remains valid for small β and large $\beta\gamma_1$. The low-temperature limit of the heat capacity (4.5) reads

$$\frac{C_V(\gamma_1)}{kN} = 1 + \frac{2-2(\delta-1)\upsilon_1^2}{\beta\gamma_1\upsilon_1^2} + \mathrm{O}\left(\frac{1}{(\beta\gamma_1\upsilon_1^2)^2}\right). \tag{4.7}$$

If $\gamma_1 \approx 1$, these expansions break down; the low-temperature expansion of $K(\delta,\beta,\gamma_1)$ in the case of small but non-vanishing υ_1 is discussed in Ref. [7]. At $\gamma_1 = 1$, the low-temperature expansions (3.20) and (3.21) apply. In this section, we consider ultra-relativistic power-law ensembles, with Lorentz factors exceeding a high-energy threshold $\gamma_1 \gg 1$.

The high-temperature expansion of the internal energy and the specific heat as stated in Eqs. (3.23)–(3.27) can also be used for $\gamma_1 > 1$, if we replace the coefficients $c_k(\delta)$ in Eq. (3.22) by

$$c_k(\delta,\gamma_1) := \frac{\gamma_1^{3-\delta+k}}{\delta-3-k}\,{}_2F_1\left(-\frac{1}{2},\frac{\delta-3-k}{2};\frac{\delta-1-k}{2};\frac{1}{\gamma_1^2}\right). \tag{4.8}$$

We note $c_k(\delta,1) = c_k(\delta)$. In the ultra-relativistic limit, $\gamma_1 \gg 1$, the hypergeometric function in $c_k(\delta,\gamma_1)$ can be dropped, cf. (A.21). However, care must be taken if the power-law exponent δ is integer, as singularities emerge in the coefficients of the hypergeometric series, cf. (A.19)–(A.23). For integers $0 \leqslant \delta \leqslant 5$ and ultra-relativistic $\gamma_1 \gg 1$, the high-temperature expansions of the internal energy read

$$\begin{aligned}
&\frac{U(\delta=0,\gamma_1)}{mN} = \frac{3}{\beta} + \frac{\beta}{2} + \mathrm{O}(\beta^2), \quad \frac{U(1,\gamma_1)}{mN} = \frac{2}{\beta} - \beta\left(\log\beta - \gamma_1^2 + \gamma_\mathrm{E} + \frac{1}{2}\right) + \mathrm{O}(\beta^2),\\
&\frac{U(2,\gamma_1)}{mN} = \frac{1}{\beta} + \gamma_1 + \beta\left(\log\beta + \gamma_\mathrm{E} - \frac{1}{2}\right) + \mathrm{O}(\beta^2), \quad \frac{U(3,\gamma_1)}{mN} = -\frac{1}{\beta}\frac{1}{\log(\beta\gamma_1) + \gamma_\mathrm{E}} + \mathrm{O}\left(\frac{1}{\log\beta}\right),\\
&\frac{U(4,\gamma_1)}{mN} = -\gamma_1(\log(\beta\gamma_1) + \gamma_\mathrm{E}) + \mathrm{O}(\beta\log^2\beta),\\
&\frac{U(5,\gamma_1)}{mN} = 2\gamma_1\left[1 + \beta\gamma_1(\log(\beta\gamma_1) + \gamma_\mathrm{E} + 1) + \mathrm{O}(\beta^2\log\beta)\right].
\end{aligned} \tag{4.9}$$

Table 2
Internal energy and heat capacities of the electronic source densities $\rho_{1,2}$ in the microquasars

	$U/(n^e mc^2)$	U (erg)	C_V (erg/K)	C_P/C_V
LS 5039				
ρ_1	6.83×10^9	5.4×10^{50}	4.0×10^{31}	1.33
ρ_2	2.79×10^6	1.7×10^{48}	3.1×10^{32}	1.33
LSI $+61°303$				
ρ_1	—	—	1.7×10^{31}	1.33
ρ_2	2.57×10^7	5.9×10^{49}	3.4×10^{31}	12.4

$U/(n^e mc^2)$ denotes the internal energy normalized with the rest mass of the respective electron population ρ_i. The internal energy U (erg) of the thermal densities $\rho_{1,2}$ in LS 5039 and ρ_1 in LSI $+61°303$ is calculated via the high-temperature expansion $U(\delta=0)$ in Eq. (3.28). The series $U(\delta=3,\gamma_1)$ in Eq. (4.9) is used for the ultra-relativistic power-law density ρ_2 of LSI $+61°303$. The input parameters $\delta=\alpha+2$, β, γ_1, and $N=n^e$ are listed in Table 1. The isochoric heat capacity is calculated by means of the series expansions $C_V(\delta=0)$ in Eq. (3.29) and $C_V(\delta=3,\gamma_1)$ in Eq. (4.10). The adiabatic index C_P/C_V is obtained from identity (3.17). The internal energy of the thermal population ρ_1 in LSI $+61°303$ remains undetermined, as the cutoff parameter β of this distribution could not be extracted from the spectral fit in Fig. 3. Regarding the ultra-relativistic power-law density ρ_2 of LSI $+61°303$, we note $\beta\gamma_1\approx1.9\times10^{-5}$, cf. Table 1, so that the quoted high-temperature expansions of internal energy and specific heat are applicable, obtained from the ultra-relativistic expansion $K(\delta=3,\beta,\gamma_1)$ listed in Eq. (A.22).

The corresponding high-temperature expansions of the ultra-relativistic heat capacity at integer power-law index $0\leqslant\delta\leqslant5$ are

$$\frac{C_V(0,\gamma_1)}{kN}=3-\frac{1}{2}\beta^2+\mathrm{O}(\beta^3),\quad \frac{C_V(1,\gamma_1)}{kN}=2+\beta^2\left(\log\beta-\gamma_1^2+\gamma_\mathrm{E}+\frac{3}{2}\right)+\mathrm{O}(\beta^3),$$
$$\frac{C_V(2,\gamma_1)}{kN}=1-\beta^2\left(\log\beta+\gamma_\mathrm{E}+\frac{1}{2}\right)+\mathrm{O}(\beta^3),\quad \frac{C_V(3,\gamma_1)}{kN}=-\frac{\log(\beta\gamma_1)+\gamma_\mathrm{E}+1}{(\log(\beta\gamma_1)+\gamma_\mathrm{E})^2}+\mathrm{O}\left(\frac{\beta}{\log^2\beta}\right),$$
$$\frac{C_V(4,\gamma_1)}{kN}=\beta\gamma_1+\mathrm{O}(\beta^2\log^2\beta),\quad \frac{C_V(5,\gamma_1)}{kN}=-2\beta^2\gamma_1^2(\log(\beta\gamma_1)+\gamma_\mathrm{E}+2)+\mathrm{O}(\beta^3\log\beta). \tag{4.10}$$

The expansions in Eqs. (4.9) and (4.10) are ultra-relativistic, terms of order $\mathrm{O}(1/\gamma_1^2)$ are systematically dropped, cf. (A.22). The high-temperature expansions valid for $\gamma_1=1$ are stated in Eqs. (3.28) and (3.29). In Table 2, we list the internal energy and heat capacities of the electron populations in the microquasars LS 5039 and LSI $+61°303$. The input parameters are inferred from the spectral fits in Figs. 1–3, as explained in the table captions.

5. Conclusion

We have investigated superluminal radiation from ultra-relativistic electron populations in γ-ray binaries and explained how to obtain the thermodynamic variables of the source densities. We demonstrated that the γ-ray spectra of the microquasars can be fitted with tachyonic cascade spectra. The spectral curvature is intrinsic and reproduced by the tachyonic spectral densities (2.1) averaged with thermal and power-law electron distributions. In Table 2, we have given estimates of the internal energy and the heat capacities of the electron plasmas in the microquasars LS 5039 and LSI $+61°303$. More generally, we have shown that Boltzmann power-law densities admit a stable and extensive entropy function (3.11). On that basis, we have derived the caloric equation of state and studied the temperature scaling of the internal energy and the heat capacities in the high-temperature regime, in particular the dependence of the scaling exponents on the electronic power-law index.

The tachyonic radiation densities (2.1) are generated by electrons in uniform motion. In Ref. [17], we studied superluminal radiation from ultra-relativistic electrons orbiting in strong magnetic fields and derived the pitch-angle scaling of the radiation densities. In the zero-magnetic-field limit, the tachyonic synchrotron densities converge to the spectral densities for uniform motion [34]. Orbital curvature induces modulations in the spectral slopes of densities (2.1), but these ripples are attenuated when performing a pitch-angle average,

cf. Figs. 1–3 in Ref. [17]. Thus we can use uniform radiation densities in the spectral fits even in the presence of magnetic fields, for instance, if the compact companion is a magnetized neutron star [1,4]. The orbital parameters of the binary system do not directly enter into the spectral fit either. If one considers microquasars as scaled-down Galactic counterparts of active galactic nuclei [2,10], one would rather expect the spectra to be determined by the global thermodynamic parameters of the electron populations in these objects, which are in turn inferred from the spectral maps, cf. Table 1.

We have focused on γ-ray spectra, which can be fitted with ultra-relativistic electron populations in the high-temperature regime. Otherwise we have to consider the quantized tachyonic spectral densities [6] instead of the classical limit (2.1). In the low-temperature regime, we also have to replace the Boltzmann power-law density in the spectral average (2.3) with its quantized fermionic counterpart. As for tachyonic X-ray spectra obtained from diffraction gratings, the tachyon mass of 2 keV has to be included in the dispersion relation, $\lambda = 2\pi/\sqrt{\omega^2 + m_{\mathrm{t}}^2}$, when parametrizing the glancing angle in the Bragg condition with energy, which affects the shape of the spectral maps in the X-ray bands. This will be discussed elsewhere.

Acknowledgements

The author acknowledges the support of the Japan Society for the Promotion of Science. The hospitality and stimulating atmosphere of the Centre for Nonlinear Dynamics, Bharathidasan University, Trichy, and the Institute of Mathematical Sciences, Chennai, are likewise gratefully acknowledged.

Appendix A. High-temperature asymptotics of Gibbs free energy and entropy

The low- and high-temperature expansions of the partition function

$$\log Z = N(\delta, \beta, V, \mu) = \frac{m^3 V}{2\pi^2} \mathrm{e}^{\beta\mu/m} K(\delta, \beta), \tag{A.1}$$

amount to deriving the $\beta \to \infty$ and $\beta \to 0$ asymptotics of the integral

$$K(\delta, \beta) := \int_1^\infty \sqrt{\gamma^2 - 1}\, \gamma^{1-\delta} \mathrm{e}^{-\beta\gamma}\, \mathrm{d}\gamma. \tag{A.2}$$

The first few orders of the low-temperature expansion read [7]

$$\log K(\delta, \beta) = -\beta \left[1 + \frac{1}{\beta} \left(\frac{3}{2} \log \beta - \frac{1}{2} \log \frac{\pi}{2} \right) + \frac{1}{\beta^2} \frac{3}{2} \left(\delta - \frac{5}{4} \right) - \frac{1}{\beta^3} \frac{3}{4} \left(\delta^2 - \frac{5}{4} \right) + \ldots \right]. \tag{A.3}$$

The high-temperature expansion is composed of two series:

$$K(\delta, \beta) = K_{\delta-2,\beta} + k_{\delta-2,\beta}, \tag{A.4}$$

where

$$K_{\delta-2,\beta} := \beta^{\delta-3} \left[\Gamma(3-\delta) - \frac{\beta^2}{2} \Gamma(1-\delta) - \frac{\beta^4}{8} \Gamma(-1-\delta) - \ldots \right]. \tag{A.5}$$

The general term of the series indicated in Eq. (A.5) is $(-)^k (1/2)_k \Gamma(3-\delta-2k) \beta^{2k}/k!$, where $(1/2)_k$ denotes the falling factorial, cf. Ref. [7]. The second series in Eq. (A.4) reads

$$k_{\delta-2,\beta} := c_0(\delta) - \beta c_1(\delta) + \frac{\beta^2}{2!} c_2(\delta) - \ldots, \tag{A.6}$$

with coefficients $c_k(\delta)$ defined in Eq. (3.22). To get an overview, we summarize the leading orders of expansion (A.4), with power-law index δ ranging in the indicated intervals:

$$K(\delta < 1, \beta) = \beta^{\delta-3} \Gamma(3-\delta) - \beta^{\delta-1} \frac{\Gamma(1-\delta)}{2} + \mathrm{O}(1, \beta^{\delta+1}),$$

$$K(1 < \delta < 3, \beta) = \beta^{\delta-3} \Gamma(3-\delta) + c_0(\delta) + \mathrm{O}(\beta^{\delta-1}),$$

$$K(3<\delta<4,\beta) = c_0(\delta) + \beta^{\delta-3}\Gamma(3-\delta) - c_1(\delta)\beta + \mathrm{O}(\beta^2),$$
$$K(4<\delta<5,\beta) = c_0(\delta) - c_1(\delta)\beta + \beta^{\delta-3}\Gamma(3-\delta) + \mathrm{O}(\beta^2),$$
$$K(\delta>5,\beta) = c_0(\delta) - c_1(\delta)\beta + \frac{c_2(\delta)}{2}\beta^2 + \mathrm{O}(\beta^4, \beta^{\delta-3}). \tag{A.7}$$

At integer δ, pole singularities emerge in the coefficients of series (A.5) and (A.6), which cancel in Eq. (A.4) if ε expanded [7]:

$$K(0,\beta) = \frac{2}{\beta^3} - \frac{1}{2\beta} + \mathrm{O}(\beta\,\log\,\beta),$$
$$K(1,\beta) = \frac{1}{\beta^2} + \frac{1}{2}\left(\log\frac{\beta}{2} + \gamma_{\mathrm{E}} - \frac{1}{2}\right) + \mathrm{O}(\beta^2\,\log\,\beta),$$
$$K(2,\beta) = \frac{1}{\beta} - \frac{\pi}{2} - \frac{\beta}{2}\left(\log\frac{\beta}{2} + \gamma_{\mathrm{E}} - \frac{3}{2}\right) + \mathrm{O}(\beta^3\,\log\,\beta),$$
$$K(3,\beta) = \log\frac{2}{\beta} - \gamma_{\mathrm{E}} - 1 + \frac{\pi}{2}\beta + \frac{\beta^2}{4}\left(\log\frac{\beta}{2} + \gamma_{\mathrm{E}} - 2\right) + \mathrm{O}(\beta^4\,\log\,\beta),$$
$$K(4,\beta) = \frac{\pi}{4} + \beta\left(\log\frac{\beta}{2} + \gamma_{\mathrm{E}}\right) - \frac{\pi}{4}\beta^2 + \mathrm{O}(\beta^3\,\log\,\beta),$$
$$K(5,\beta) = \frac{1}{3} - \frac{\pi}{4}\beta - \frac{\beta^2}{2}\left(\log\frac{\beta}{2} + \gamma_{\mathrm{E}} - \frac{1}{2}\right) + \mathrm{O}(\beta^3). \tag{A.8}$$

γ_{E} is Euler's constant. At integer $\delta<0$ and $\delta>5$, expansions $K(\delta<1,\beta)$ and $K(\delta>5,\beta)$ in Eq. (A.7) can be used, as the indicated orders are singularity free. This settles the high-temperature expansion of the partition function (A.1) for arbitrary power-law index δ.

The high-temperature expansion of the chemical potential (3.9), the Helmholtz free energy (3.12) and the Gibbs potential $F + PV$,

$$G(\delta,\beta,P,N) = -\frac{mN}{\beta}\log\left(\frac{m^4}{2\pi^2 P}\,\frac{K(\delta,\beta)}{\beta}\right), \tag{A.9}$$

are obtained from the $\log K(\delta,\beta)$ series, which reads in the respective δ-range as

$$\log K(\delta<1,\beta) = (\delta-3)\log\,\beta + \log\,\Gamma(3-\delta) - \frac{\beta^2}{2(2-\delta)(1-\delta)} + \mathrm{O}(\beta^4, \beta^{3-\delta}),$$
$$\log K(1<\delta<3,\beta) = (\delta-3)\log\,\beta + \log\,\Gamma(3-\delta) + \frac{c_0(\delta)}{\Gamma(3-\delta)}\beta^{3-\delta} + \mathrm{O}(\beta^2, \beta^{2(3-\delta)}),$$
$$\log K(3<\delta<4,\beta) = \log\,c_0(\delta) + \frac{\Gamma(3-\delta)}{c_0(\delta)}\beta^{\delta-3} - \frac{c_1(\delta)}{c_0(\delta)}\beta - \frac{\Gamma^2(3-\delta)}{2c_0^2(\delta)}\beta^{2(\delta-3)} + \mathrm{O}(\beta^{\delta-2}),$$
$$\log K(4<\delta<5,\beta) = \log\,c_0(\delta) - \frac{c_1(\delta)}{c_0(\delta)}\beta + \frac{\Gamma(3-\delta)}{c_0(\delta)}\beta^{\delta-3} + \mathrm{O}(\beta^2),$$
$$\log K(\delta>5,\beta) = \log\,c_0(\delta) - \frac{c_1(\delta)}{c_0(\delta)}\beta + \frac{\beta^2}{2}\left(\frac{c_2(\delta)}{c_0(\delta)} - \frac{c_1^2(\delta)}{c_0^2(\delta)}\right) + \mathrm{O}(\beta^3, \beta^{\delta-3}). \tag{A.10}$$

Internal energy and specific heat are found by term-by-term differentiation of the $\log K$ series. For integers $0\leqslant\delta\leqslant5$, singularities occur in the series coefficients in Eq. (A.10). In this case, we use (A.8) to find

$$\log\,K(0,\beta) = -3\,\log\,\beta + \log\,2 - \frac{1}{4}\beta^2 + \mathrm{O}(\beta^4\,\log\,\beta),$$
$$\log\,K(1,\beta) = -2\,\log\,\beta + \frac{\beta^2}{2}\left(\log\frac{\beta}{2} + \gamma_{\mathrm{E}} - \frac{1}{2}\right) + \mathrm{O}(\beta^4\,\log\,\beta),$$

$$\log K(2,\beta) = -\log\beta - \frac{\pi}{2}\beta - \frac{\beta^2}{2}\left(\log\frac{\beta}{2} + \gamma_{\rm E} - \frac{3}{2} + \frac{\pi^2}{4}\right) + {\rm O}(\beta^3\log\beta),$$

$$\log K(3,\beta) = \log\left(\log\frac{2}{\beta} - \gamma_{\rm E} - 1\right) - \frac{\pi}{2}\frac{\beta}{\log(\beta/2) + \gamma_{\rm E} + 1} + {\rm O}(\beta^2),$$

$$\log K(4,\beta) = \log\frac{\pi}{4} + \beta\frac{4}{\pi}\left(\log\frac{\beta}{2} + \gamma_{\rm E}\right) + {\rm O}(\beta^2\log^2\beta),$$

$$\log K(5,\beta) = -\log 3 - \frac{3\pi}{4}\beta - \frac{3}{2}\beta^2\left(\log\frac{\beta}{2} + \gamma_{\rm E} - \frac{1}{2} + \frac{3\pi^2}{16}\right) + {\rm O}(\beta^3\log\beta). \tag{A.11}$$

The high-temperature expansion of the entropy function (3.11) is obtained by substituting the asymptotic series of the caloric equation of state and the chemical potential into

$$S(\delta,\beta,V,N) = kN\left(1 + \beta\frac{U}{mN} - \beta\frac{\mu}{m}\right). \tag{A.12}$$

Alternatively, we may use the $\log K$ series in Eqs. (A.10) and (A.11) and term-by-term differentiation to find the $\beta\to 0$ asymptotics of S, starting with

$$\frac{S}{kN} = 1 + \log\frac{m^3V}{2\pi^2N} + \frac{S_0}{kN}, \quad \frac{S_0}{kN} := -\beta^2\frac{\partial}{\partial\beta}\frac{\log K(\delta,\beta)}{\beta}. \tag{A.13}$$

We note the leading-order asymptotics

$$\frac{S_0(\delta<3)}{kN} \sim (3-\delta)\log\frac{1}{\beta} + \log\Gamma(3-\delta) + 3 - \delta, \tag{A.14}$$

and S_0 approaches a finite limit, $S_0 \sim kN\log c_0(\delta)$, for $\delta>3$, cf. (A.10). At $\delta = 3$, S_0 has a double-logarithmic divergence in the high-temperature limit, cf. (A.11).

We finally discuss the low- and high-temperature asymptotics of the ultra-relativistic partition function, cf. (4.1):

$$Z = \sum_{n=0}^{\infty}\frac{1}{n!}\left(\int_V\int_{H\geqslant H_1}(H/m)^{-\delta}{\rm e}^{-\beta H/m-\alpha}\frac{{\rm d}^3p}{(2\pi)^3}{\rm d}^3q\right)^n. \tag{A.15}$$

We find $\log Z$ as in Eq. (A.1), with $K(\delta,\beta)$ replaced by

$$K(\delta,\beta,\gamma_1) := \int_{\gamma_1}^{\infty}\sqrt{\gamma^2-1}\gamma^{1-\delta}{\rm e}^{-\beta\gamma}\,{\rm d}\gamma, \tag{A.16}$$

so that

$$\frac{N}{V} = \frac{m^3}{2\pi^2}{\rm e}^{\beta\mu/m}K(\delta,\beta,\gamma_1). \tag{A.17}$$

Here, N is to be identified with the renormalized electron count $n_1^{\rm e}$ as defined after (2.5), and the power-law exponent δ is related to the electron index α defined in Eq. (2.2) by $\delta = \alpha + 2$. The low-temperature expansions of the chemical potential (3.9) and the free energies (3.12) and (A.9) are obtained by substituting [7]

$$\log K(\delta,\beta,\gamma_1) = -\beta\gamma_1 + \log\frac{\gamma_1^{2-\delta}\upsilon_1}{\beta} + \frac{1-(\delta-1)\upsilon_1^2}{\beta\gamma_1\upsilon_1^2} + {\rm O}\left(\frac{1}{(\beta\gamma_1\upsilon_1^2)^2}\right), \tag{A.18}$$

where $\upsilon_1 = \sqrt{1-1/\gamma_1^2}$.

It remains to settle the high-temperature limit, the $\beta\to 0$ asymptotics of $K(\delta,\beta,\gamma_1)$ in Eq. (A.16). As in Eq. (A.4), the expansion is composed of two series [7]:

$$K(\delta,\beta,\gamma_1) = K_{\delta-2,\beta} + f_{\delta-2,\beta}, \tag{A.19}$$

where series $K_{\delta-2,\beta}$ is defined in Eq. (A.5) and

$$f_{\delta-2,\beta}(\gamma_1) := \sum_{k=0}^{\infty} \frac{(-)^k \beta^k}{k!} c_k(\delta,\gamma_1), \tag{A.20}$$

with coefficients $c_k(\delta,\gamma_1)$ defined in Eq. (4.8). The high-temperature expansion of $\log K(\delta,\beta,\gamma_1)$ reads as stated in Eq. (A.10) for $\log K(\delta,\beta)$, with coefficients $c_k(\delta)$ replaced by $c_k(\delta,\gamma_1)$. In the ultra-relativistic limit, we can use the hypergeometric series in Eq. (4.8):

$$c_k(\delta,\gamma_1) = \frac{\gamma_1^{3-\delta+k}}{\delta-3-k}\left(1 - \frac{1}{2}\frac{\delta-3-k}{\delta-1-k}\frac{1}{\gamma_1^2} + \mathrm{O}\left(\frac{1}{\gamma_1^4}\right)\right), \tag{A.21}$$

so that the expansion parameter of series $f_{\delta-2,\beta}$ in Eq. (A.20) is $\beta\gamma_1$. If $\beta\gamma_1 \gg 1$, despite of β being small, the low-temperature expansion (A.18) applies.

At integer δ, the coefficients $c_k(\delta,\gamma_1)$ in Eq. (A.20) become singular owing to poles in the coefficients of the hypergeometric series. They can be dealt with by ε expansion and are canceled by corresponding poles of $K_{\delta-2,\beta}$ in Eq. (A.19), which arise in the Γ-functions in Eq. (A.5). In the ultra-relativistic limit, $\gamma_1 \gg 1$ (but still $\beta\gamma_1 \ll 1$), we find, for integers $0 \leqslant \delta \leqslant 5$,

$$\begin{aligned}
K(\delta=0,\beta,\gamma_1) &= \frac{2}{\beta^3} - \frac{1}{2\beta} + \mathrm{O}(\beta\log\beta) \\
&\quad - \gamma_1^3\left[\frac{1}{3} + \mathrm{O}\left(\frac{1}{\gamma_1^2}\right) - \frac{\beta\gamma_1}{4}\left(1+\mathrm{O}\left(\frac{1}{\gamma_1^2}\right)\right) + \frac{\beta^2\gamma_1^2}{10}\left(1+\mathrm{O}\left(\frac{1}{\gamma_1^2}\right)\right) + \mathrm{O}\left(\beta^3\gamma_1^3\right)\right], \\
K(1,\beta,\gamma_1) &= \frac{1}{\beta^2} + \frac{1}{2}\left(\log\beta + \gamma_{\mathrm{E}}\right) + \mathrm{O}\left(\beta^2\log\beta\right) \\
&\quad - \gamma_1^2\left[\frac{1}{2} + \mathrm{O}\left(\frac{\log\gamma_1}{\gamma_1^2}\right) - \frac{\beta\gamma_1}{3}\left(1+\mathrm{O}\left(\frac{1}{\gamma_1^2}\right)\right) + \frac{\beta^2\gamma_1^2}{8}\left(1+\mathrm{O}\left(\frac{1}{\gamma_1^2}\right)\right) + \mathrm{O}\left(\beta^3\gamma_1^3\right)\right], \\
K(2,\beta,\gamma_1) &= \frac{1}{\beta} - \frac{\beta}{2}\left(\log\beta + \gamma_{\mathrm{E}} - 1\right) + \mathrm{O}\left(\beta^3\log\beta\right) \\
&\quad - \gamma_1\left[1 + \mathrm{O}\left(\frac{1}{\gamma_1^2}\right) - \frac{\beta\gamma_1}{2}\left(1+\mathrm{O}\left(\frac{\log\gamma_1}{\gamma_1^2}\right)\right) + \frac{\beta^2\gamma_1^2}{6}\left(1+\mathrm{O}\left(\frac{1}{\gamma_1^2}\right)\right) + \mathrm{O}\left(\beta^3\gamma_1^3\right)\right], \\
K(3,\beta,\gamma_1) &= -\log\beta - \gamma_{\mathrm{E}} + \frac{\beta^2}{4}\left(\log\beta + \gamma_{\mathrm{E}} - \frac{3}{2}\right) + \mathrm{O}\left(\beta^4\log\beta\right) \\
&\quad - \log\gamma_1 + \mathrm{O}\left(\frac{1}{\gamma_1^2}\right) + \beta\gamma_1\left(1+\mathrm{O}\left(\frac{1}{\gamma_1^2}\right)\right) - \frac{\beta^2\gamma_1^2}{4}\left(1+\mathrm{O}\left(\frac{\log\gamma_1}{\gamma_1^2}\right)\right) + \mathrm{O}\left(\beta^3\gamma_1^3\right), \\
K(4,\beta,\gamma_1) &= \beta\left(\log\beta + \gamma_{\mathrm{E}} - 1\right) + \mathrm{O}\left(\beta^3\log\beta\right) \\
&\quad + \frac{1}{\gamma_1}\left[1 + \mathrm{O}\left(\frac{1}{\gamma_1^2}\right) + \beta\gamma_1\left(\log\gamma_1 + \mathrm{O}\left(\frac{1}{\gamma_1^2}\right)\right) - \frac{\beta^2\gamma_1^2}{2}\left(1+\mathrm{O}\left(\frac{1}{\gamma_1^2}\right)\right) + \mathrm{O}\left(\beta^3\gamma_1^3\right)\right], \\
K(5,\beta,\gamma_1) &= -\frac{\beta^2}{2}\left(\log\beta + \gamma_{\mathrm{E}} - \frac{3}{2}\right) + \mathrm{O}\left(\beta^4\log\beta\right) \\
&\quad + \frac{1}{\gamma_1^2}\left[\frac{1}{2} + \mathrm{O}\left(\frac{1}{\gamma_1^2}\right) - \beta\gamma_1\left(1+\mathrm{O}\left(\frac{1}{\gamma_1^2}\right)\right) - \frac{\beta^2\gamma_1^2}{2}\left(\log\gamma_1 + \mathrm{O}\left(\frac{1}{\gamma_1^2}\right)\right) + \mathrm{O}\left(\beta^3\gamma_1^3\right)\right].
\end{aligned} \tag{A.22}$$

There are two expansion parameters in these series, β in $K_{\delta-2,\beta}$ and $\beta\gamma_1$ in $f_{\delta-2,\beta}$, cf. (A.19). It is possible to perform a systematic high-temperature expansion in β, keeping γ_1 fixed and assuming $\beta \to 0$, just by reordering

the terms in Eq. (A.22):

$$\log K(0,\beta,\gamma_1) = -3\log\beta + \log 2 - \frac{1}{4}\beta^2 + \mathrm{O}(\beta^3),$$
$$\log K(1,\beta,\gamma_1) = -2\log\beta + \frac{\beta^2}{2}(\log\beta - \gamma_1^2 + \gamma_\mathrm{E}) + \mathrm{O}(\beta^3),$$
$$\log K(2,\beta,\gamma_1) = -\log\beta - \beta\gamma_1 - \frac{\beta^2}{2}(\log\beta + \gamma_\mathrm{E} - 1) + \mathrm{O}(\beta^3),$$
$$\log K(3,\beta,\gamma_1) = \log\big(-\log(\beta\gamma_1) - \gamma_\mathrm{E}\big) - \frac{\beta\gamma_1}{\log(\beta\gamma_1) + \gamma_\mathrm{E}} + \mathrm{O}(\beta^2),$$
$$\log K(4,\beta,\gamma_1) = -\log\gamma_1 + \beta\gamma_1\big(\log(\beta\gamma_1) + \gamma_\mathrm{E} - 1\big) + \mathrm{O}(\beta^2\log^2\beta),$$
$$\log K(5,\beta,\gamma_1) = -\log(2\gamma_1^2) - 2\beta\gamma_1 - \beta^2\gamma_1^2\left(\log(\beta\gamma_1) + \gamma_\mathrm{E} + \frac{1}{2}\right) + \mathrm{O}(\beta^3\log\beta). \tag{A.23}$$

Here, we have dropped the $\mathrm{O}(1/\gamma_1^2)$ estimates indicated in Eq. (A.22). These expansions are valid in the ultra-relativistic regime, $\gamma_1 \gg 1$, provided that β is sufficiently small to ensure $\beta\gamma_1 \ll 1$.

The ultra-relativistic high-temperature asymptotics of entropy is obtained by means of (A.13), with $K(\delta,\beta)$ replaced by $K(\delta,\beta,\gamma_1)$ in the reduced entropy function S_0. For power-law indices $\delta \leqslant 3$, the leading order of S_0 is independent of the ultra-relativistic threshold γ_1, cf. (A.23), so that the high-temperature limit of S_0 in Eq. (A.14) remains unchanged. For power-law indices $\delta > 3$, the reduced entropy admits a finite limit, $S_0(\beta \to 0) \sim kN\log c_0(\delta,\gamma_1)$, cf. (A.10) and (A.21).

References

[1] M.V. McSwain, et al., Astrophys. J. 600 (2004) 927.
[2] J. Casares, et al., Mon. Not. R. Astron. Soc. 364 (2005) 899.
[3] J. Casares, et al., Mon. Not. R. Astron. Soc. 360 (2005) 1105.
[4] E.D. Grundstrom, et al., Astrophys. J. 656 (2007) 437.
[5] R. Tomaschitz, Physica A 320 (2003) 329.
[6] R. Tomaschitz, Eur. Phys. J. C 49 (2007) 815.
[7] R. Tomaschitz, Ann. Phys. 322 (2007) 677.
[8] B.A. Harmon, et al., Astrophys. J. Suppl. 154 (2004) 585.
[9] V. Bosch-Ramon, J.M. Paredes, Chin. J. Astron. Astrophys. 5 (Suppl.) (2005) 133.
[10] V. Bosch-Ramon, J.M. Paredes, Astron. Astrophys. 417 (2004) 1075.
[11] F. Aharonian, et al., Astron. Astrophys. 460 (2006) 743.
[12] R. van Dijk, et al., Astron. Astrophys. 315 (1996) 485.
[13] D.A. Kniffen, et al., Astrophys. J. 486 (1997) 126.
[14] V. Bosch-Ramon, J.M. Paredes, Astron. Astrophys. 425 (2004) 1069.
[15] J. Albert, et al., Science 312 (2006) 1771.
[16] R. Tomaschitz, Astropart. Phys. 27 (2007) 92.
[17] R. Tomaschitz, Phys. Lett. A 366 (2007) 289.
[18] J.M. Paredes, V. Bosch-Ramon, G.E. Romero, Astron. Astrophys. 451 (2006) 259.
[19] M. Chernyakova, A. Neronov, R. Walter, Mon. Not. R. Astron. Soc. 372 (2006) 1585.
[20] L. Sidoli, et al., Astron. Astrophys. 459 (2006) 901.
[21] R. Tomaschitz, Eur. Phys. J. D 32 (2005) 241.
[22] R. Tomaschitz, J. Phys. A 38 (2005) 2201.
[23] J.M. Fierro, et al., Astrophys. J. 494 (1998) 734.
[24] S.P. Reynolds, J.W. Keohane, Astrophys. J. 525 (1999) 368.
[25] I. de Pater, et al., Icarus 163 (2003) 434.
[26] K. Tsuchiya, et al., Astrophys. J. 606 (2004) L115.
[27] C. Itoh, et al., Astron. Astrophys. 462 (2007) 67.
[28] R. Tomaschitz, Physica A 335 (2004) 577.
[29] R. Tomaschitz, Astropart. Phys. 23 (2005) 117.
[30] F. Aharonian, et al., Astron. Astrophys. 430 (2005) 865.
[31] R. Enomoto, et al., Astrophys. J. 652 (2006) 1268.
[32] S. Chandrasekhar, An Introduction to the Study of Stellar Structure, Dover, New York, 1967.
[33] H.B. Callen, Thermodynamics and an Introduction to Thermostatistics, Wiley, New York, 1987.
[34] R. Tomaschitz, Eur. Phys. J. C 45 (2006) 493.